

Supporting Information
Bryce, Boisbouvier, Bax

Table 1S: Experimental (D_{meas}) and predicted (D_{calc}) residual dipolar couplings, $(^1J + ^1D)^{(18.8\text{ T})} - (^1J + ^1D)^{(11.75\text{ T})}$, for the Dickerson dodecamer. All couplings are one-bond C-H RDCs. The predicted values are the result of a singular-value decomposition fit to the 1NAJ PDB structure. The experimental rms noise determined from peak widths and signal-to-noise is 0.342 Hz and the rms deviation between the measured and calculated values is 0.495 Hz. This latter value corresponds to a Q factor of 0.417.

Nucleotide	Carbon atom	$D_{\text{meas}} / \text{Hz}$	Magnitude of expt error / Hz	$D_{\text{calc}} / \text{Hz}$
5	C2	-1.0899	0.2440	-1.2642
6	C2	-0.8579	0.2442	-1.2434
1	C5	-1.0369	0.1377	-0.8543
3	C5	-1.4038	0.2287	-1.1765
9	C5	-1.6988	0.2314	-1.3954
11	C5	-1.1059	0.1959	-1.2612
1	C6	-0.9748	0.2052	-1.2008
3	C6	-1.7088	0.3278	-1.3280
7	C6	-2.2057	0.5327	-1.3844
8	C6	-2.3107	0.5130	-1.3035
9	C6	-1.3138	0.3396	-1.2619
11	C6	-1.8018	0.3155	-1.3789
2	C8	-1.0419	0.2269	-1.4053
4	C8	-1.9797	0.2600	-1.2681
10	C8	-1.5738	0.2171	-1.2600
12	C8	-1.3578	0.1558	-1.1593
1	C1'	-0.7089	0.1221	-0.2704
4	C1'	-0.7989	0.3123	-1.2899
5	C1'	-0.6429	0.3030	-1.2448
7	C1'	-1.2758	0.2496	-0.9761
8	C1'	-1.4728	0.2806	-1.3407
11	C1'	-0.7389	0.1507	-1.0816
1	C3'	0.0207	0.1806	-0.0262
5	C3'	-0.5895	0.3857	-0.8262
6	C3'	-0.4162	0.4034	-0.9324
8	C3'	-0.3350	0.4186	-0.9421
9	C3'	-0.7128	0.2880	-0.9984
11	C3'	-0.7091	0.2734	-0.6325
12	C3'	-0.7158	0.1611	-0.9633
1	C4'	0.2038	0.1843	0.3369
5	C4'	-0.9312	0.6163	-0.1616
6	C4'	1.0581	0.6853	-0.1229
7	C4'	0.4552	0.7603	-0.1494
8	C4'	-1.2272	0.3509	-0.1922
12	C4'	-0.6371	0.2343	-0.8810

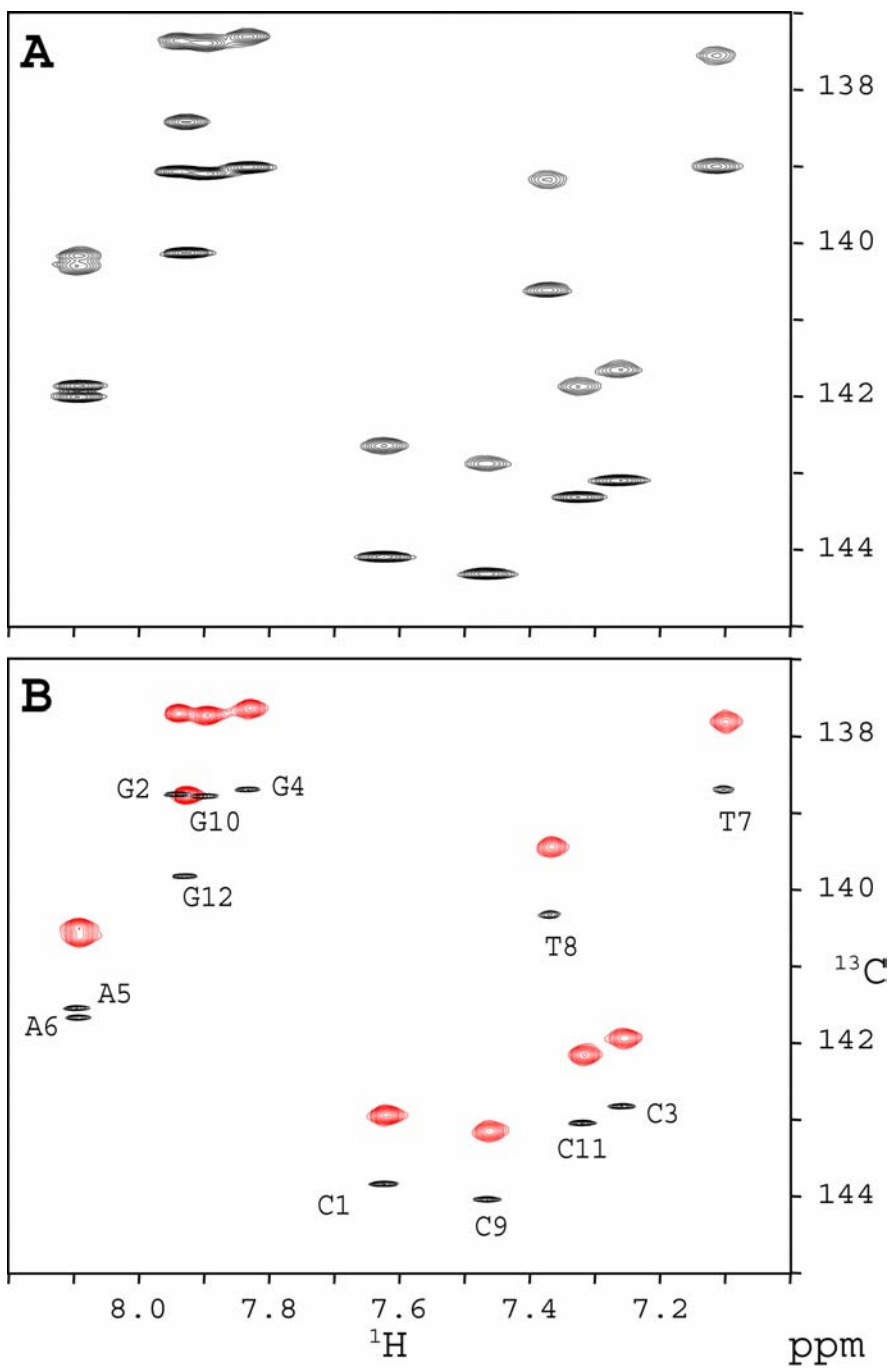


Figure 1S. See caption on following page.

Figure 1S: NMR spectra of the Dickerson dodecamer displaying the splittings for pyrimidine C₆ and purine C₈ nuclei at 11.75 T (**A**) and 18.8 T (**B**). Spectra have been recorded at T = 35°C using a sample containing 4 mM unlabeled d(CGCGAATTCGCG)₂, 50 mM KCl, 1 mM EDTA, and 10 mM potassium phosphate buffer (pH=7.0) in 99.9% D₂O, in a 270 μL Shigemi microcell. Spectrum **A** is a coupled HSQC recorded using a Bruker DRX spectrometer equipped with a cryogenic triple resonance pulsed field gradient probehead. The Boltzmann ¹³C polarization has been suppressed at the beginning of the pulse sequence using a ¹³C 90° pulse followed by a gradient. Total measuring time is 21h, for a time domain matrix of 512* × 1024* data points, with acquisition times of 102 ms (t₁) and 73 ms (t₂). Due to significant cross-correlation effects at high field (Boisbouvier, J., Brutscher, B., Simorre, J.-P., Marion, D. (1999) *J. Biomol. NMR*, **14**, 241-252), different optimization of the acquisition times is required for the selection of aromatic carbon upfield and downfield components. Panel **B** corresponds to the superimposition of two spin-state-selective experiments (using a non-CT version of the pulse scheme published in Boisbouvier, J., Brutscher, B., Pardi, A., Marion, D., Simorre, J.-P. (2000) *J. Am. Chem. Soc.*, **122**, 6779-6780). The spectrum for the carbon downfield component (TROSY) is shown in black. Total measuring time is 19h, for a time domain matrix of 1024* × 1024* data points, with acquisition times of 205 ms (t₁) and 85 ms (t₂). The spectrum for the carbon upfield component (*anti*-TROSY) is shown in red. Total measuring time is 24h, for a time domain matrix of 205* × 1024* data points, with acquisition times of 41 ms (t₁) and 85 ms (t₂). Assignments are indicated on panel B for the ¹³C downfield component.

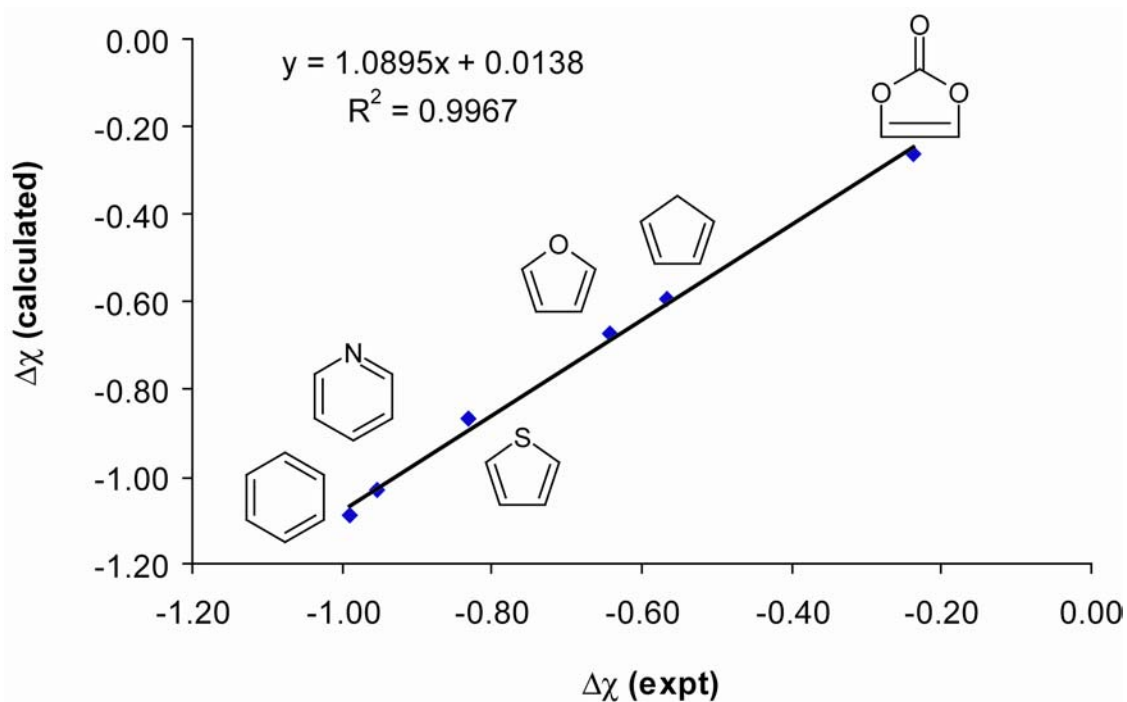


Figure 2S. Correlation between B3LYP/6-311++G(3df,3pd) calculated magnetic susceptibility anisotropies and precise gas-phase (single-crystal in the case of benzene) experimental data.¹ Units are $10^{-27} \text{ J T}^{-2}$. Atomic coordinates were obtained by geometry optimization at the same level of theory. These molecules were chosen as a suitable test set for the calculation of magnetic susceptibility anisotropies of planar molecules following Ruud et al.²

¹ Flygare, W. H. *Chem. Rev.* **1974**, *74*, 653-687.

² Ruud, K.; Skaane, H.; Helgaker, T.; Bak, K. L.; Jorgensen, P. *J. Am. Chem. Soc.* **1994**, *116*, 10135-10140.

Table 2S: Calculated magnetic susceptibility tensor anisotropies (units: 10^{-27} J T $^{-2}$) and rhombicities for the nucleic acid bases. Geometries are from Clowney, L.; Jain, S. C.; Srinivasan, A. R.; Westbrook, J.; Olson, W. K.; Berman, H. M. *J. Am. Chem. Soc.* **1996**, *118*, 509-518.

Computational method	B3LYP/ 6-311++G(3df,3pd)		RHF/ 6-311++G(3df,3pd)	
	$\Delta\chi$	R	$\Delta\chi$	R
Cytosine	-0.387	0.06	-0.406	0.14
Thymine	-0.406	0.38	-0.385	0.42
Uracil	-0.366	0.16	-0.352	0.20
Adenine	-1.296	0.03	-1.301	0.06
Guanine	-0.915	0.15	-0.932	0.14

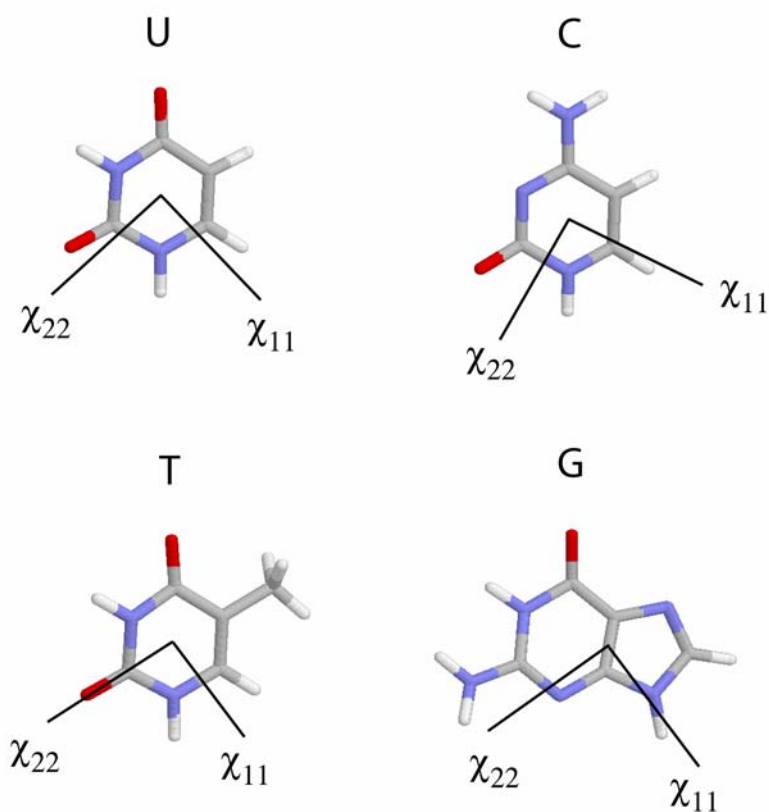


Figure 3S: Orientations of the principal axis systems of the nucleic acid base magnetic susceptibility tensors. The pseudo-unique χ_{33} component lies perpendicular to the molecular plane in all cases. For guanine, thymine, and uracil, χ_{22} is oriented approximately along the N3-C4 bond (within 3° in guanine, within 9° in thymine, within 12° in uracil). For cytosine, χ_{11} bisects the C2-N3-C4 angle (within 3°). The angles quoted above refer specifically to the calculated tensors described in Table 1 of the main text. In adenine, the rhombicity approaches zero and the calculated orientations of the in-plane components become meaningless.

Table 3S: Calculated magnetic susceptibility tensor anisotropies and rhombicities (B3LYP/6-311++G(3df,3pd)) for the primary contributors to protein magnetic susceptibility. Geometries used were optimized at the B3LYP/6-311++G(3df,3pd) level. The pseudo-unique χ_{33} component lies perpendicular to the molecular plane (peptide plane or ring plane) in all cases.

	Model used in calculation	$\Delta\chi / 10^{-27} \text{ J T}^{-2}$
Peptide bond	formamide	-0.100
Histidine sidechain	imidazole	-0.749
Tyrosine sidechain	phenol	-0.979
Tryptophan sidechain	indole	-1.772
Phenylalanine sidechain	benzene	-1.087

Table 4S: Nucleic acid base magnetic susceptibility anisotropies used to produce the “Literature” results given in Table 2. Units are $10^{-27} \text{ J T}^{-2}$.

	Skoglund ³	Zhang et al. ⁴	van Buuren et al. ⁵
Cytosine	-0.28	-0.94	-1.03
Thymine	-0.13	-0.94	-1.03
Uracil	-0.13	-0.94	-1.03
Adenine	-1.52	-1.52	-1.03
Guanine	-0.90	-1.46	-1.03
Average per base (C,G,A,T or C,G,A,U)	-0.708	-1.22	-1.03

³ Skoglund, C. M. Thesis, Carnegie-Mellon University, Pittsburgh, 1987. No value for uracil is reported; we have used the reported value for thymine.

⁴ Zhang, Q.; Throolin, R.; Pitt, S. W.; Serganov, A.; Al-Hashimi, H. M. *J. Am. Chem. Soc.* **2003**, *125*, 10530-10531. An explicit value for thymine is not given; however, the value of $-0.94 \times 10^{-27} \text{ J T}^{-2}$ is given as a standard value for the other pyrimidines (C, U), independent of ring substituents.

⁵ van Buuren, B. N. M.; Schleucher, J.; Wittmann, V.; Griesinger, C.; Schwalbe, H.; Wijmenga, S. S. *Angew. Chem. Int. Ed.* **2004**, *43*, 187-192.

Table 5S: Calculated magnetic susceptibility tensor anisotropies (B3LYP/6-311+G*) for a series of sugar-phosphate conformers. In all cases, the model consisted of the atoms for a given sugar, from C5'(i) to O3'(i), and the PO₃ group from the next residue (i+1). C5'(i) and O5'(i+1) were saturated with protons (see Figure 4S). In this model, all atoms of the sugar-phosphate moiety are included once, with no repetition. All angles are given in degrees. Labels follow the system of Murray et al., except for the deoxyribose models for which the labels correspond to the nucleotide numbering in the Dickerson dodecamer.

label	sugar	P	ψ_m	ϵ	ζ	$\frac{\Delta\chi}{10^{-27} \text{ J T}^{-2}}$	R	Source of coordinates
2'em	ribose	162	35	-100	-70	-0.133	0.16	Murray et al. ⁶
2'et	ribose	162	35	-120	175	-0.124	0.09	Murray et al.
2'ep	ribose	162	35	-100	85	-0.147	0.25	Murray et al.
C3	deoxyribose	124	32	-164	-97	+0.104	0.11	Wu et al. ⁷
A5	deoxyribose	145	34	-175	-103	+0.108	0.25	Wu et al.
T7	deoxyribose	109	34	-178	-88	+0.087	0.14	Wu et al.
G10	deoxyribose	156	35	-170	-114	+0.114	0.43	Wu et al.
3'em	ribose	18	35	-150	-75	+0.098	0.44	Murray et al.
3'et	ribose	18	35	-140	175	+0.088	0.64	Murray et al.
3'e-140	ribose	18	35	-125	-140	-0.087	0.52	Murray et al.
3'ep	ribose	18	35	-150	45	+0.093	0.45	Murray et al.

⁶ Structures were generated according to the angles given in Murray, L., J. W.; Arendal III, B.; Richardson, D. C.; Richardson, J. S. *Proc. Natl. Acad. Sci. USA* **2003**, *100*, 13904-13909 using the Dynamo Molecular Structure Engine (F. Delaglio, <http://spin.niddk.nih.gov/NMRPipe/dynamo/>).

⁷ Coordinates were taken from the 1NAJ pdb file (model 3) for the Dickerson dodecamer, see: Wu, Z.; Delaglio, F.; Tjandra, N.; Zhurkin, V. B.; Bax, A. *J. Biomol. NMR* **2003**, *26*, 297-315.

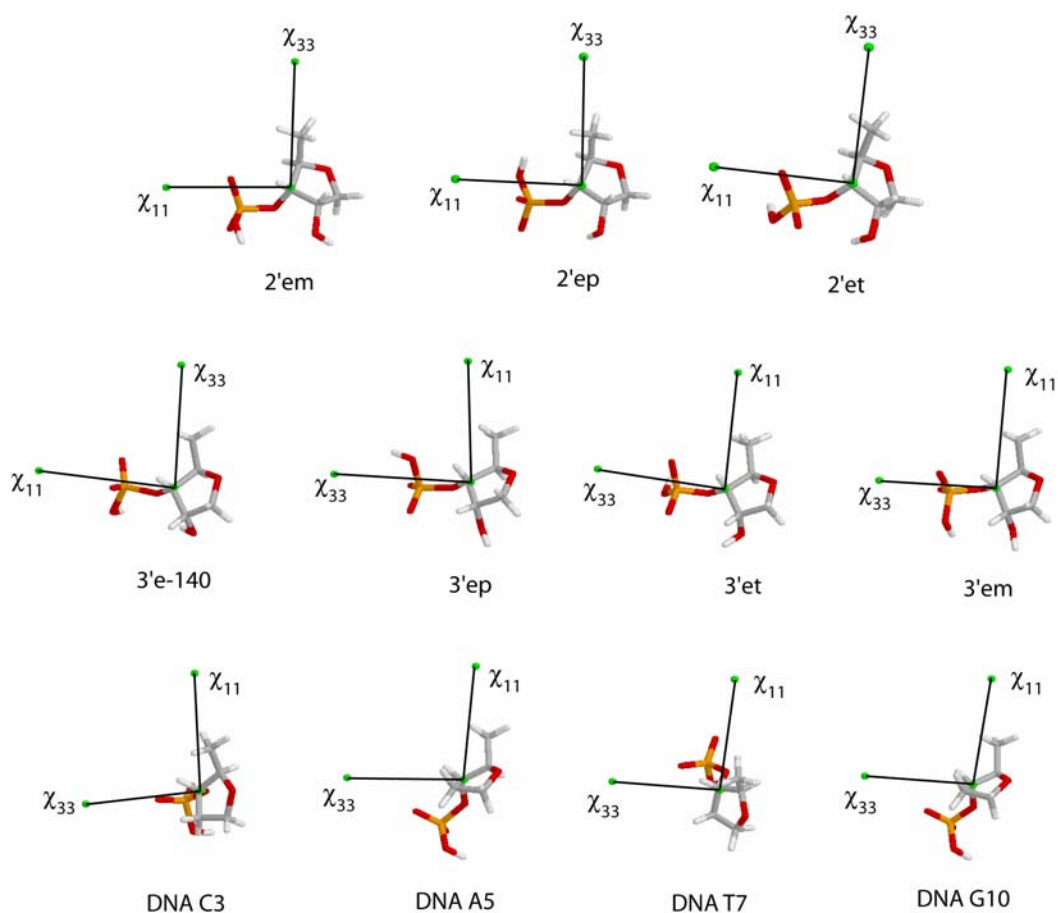


Figure 4S: Calculated (B3LYP/6-311+G*) magnetic susceptibility tensor orientations for the models listed in Table 5S. The view in each case is approximately along the χ_{22} principal axis. Importantly, the orientations vary considerably for the four nominally “C2’-endo” sugar-phosphate conformers taken directly from the DNA 1NAJ pdb file (model 3).